Optimized Fast Convolution based Filtered-OFDM Processing for 5G

Juha Yli-Kaakinen, Toni Levanen, Markku Renfors, and Mikko Valkama
Dept. of Electronics and Communications Engineering, Tampere University of Technology, Finland
{juha.yli-kaakinen, toni.levanen, markku.renfors, mikko.e.valkama}@tut.fi

***Abstract*—This paper investigates the application of flexible fast-convolution (FC) filtering scheme for multiplexing orthogonal frequency-division multiplexing (OFDM) physical resource blocks (PRBs) in a spectrally well-localized manner. This scheme is able to suppress interference leakage between adjacent PRBs, thus supporting independent waveform parametrization and numerologies for different PRBs, as well as asynchronous multiuser operation. These are considered as important features in the 5G waveform development. This contribution focuses on optimizing FC based OFDM transmultiplexers such that the in-band interference is minimized subject to the given out-of-band emission constraint. The performance of the optimized designs is demonstrated using resource block groups (RBGs) of different sizes and with various design parameters. The proposed scheme has great flexibility in tuning the filtering bandwidths dynamically according the resource allocation to different users with different requirements regarding the OFDM waveform numerology. Also the computational complexity is competitive with existing time-domain windowing approaches and becomes superior when the number of filtering bands is increased.**

Keywords*—*waveforms, multicarrier, filtered-OFDM, fast-convolution, 5G

I. Introduction

ORTHOGONAL frequency-division multiplexing (ODFM) is extensively utilized in modern broadband radio access systems. This is due to the simple and robust way of channel equalization, high flexibility and efficiency in allocating spectral resources to different users, as well as simplicity of combining multiantenna schemes with the core functionality [2]. However, OFDM has major limitations in challenging new spectrum use scenarios, like asynchronous multiple access and mixed numerology cases aiming to use adjustable subcarrier spacings (SCSs), symbol lengths, and cyclic prefixes (CPs), depending on the service requirements.

Among various advanced waveform candidates, filtered OFDM schemes are receiving increasing attention in the 5th generation (5G) waveform development, due to their ability to address the mentioned issues while maintaining high level of commonality with legacy OFDM systems. Generally, these schemes apply filtering at subband level, over a resource block group (RBG) including one or more physical resource blocks (PRBs). In fact Phase 1 standardization of 5G in 3GPP is expected to choose CP-OFDM as the basis of enhanced mobile broadband (eMBB) services, with time-domain windowing or subband filtering as alternative means for spectrum enhancement [3]. Time-domain windowing has low complexity but limited capability for spectrum enhancement. Therefore, it is particularly interesting investigate effective and flexible filtered OFDM schemes.

In the existing studies, time-domain windowing based processing [4], [5], or effective uniform polyphase filter bank (FB) structures [6] have been considered. In our recent study, flexible and effective fast-convolution (FC) filtering scheme was proposed for filtered OFDM in [7] whereas the possibility to design parametrizations supporting adjustable CP lengths while the overall CP-OFDM symbol duration remains constant was demonstrated in [8].

In this paper, we first derive the analytical models for the FC based synthesis and analysis FBs and extend these models for the FC-filtered OFDM waveform. By using these models, the in-band interference (IBI) and the out-of-band emission (OBE) of the FC-filtered OFDM can be easily evaluated. Then the FC based transmultiplexer design problem is formulated as an optimization problem. In this problem the goal is to minimize the maximum of the IBI subject to the given OBE constraint.

The simulation results show that the proposed approach is feasible for spectrum allocations of different sizes and for adjustable SCSs. Furthermore, the configuration can be dynamically adjusted in accordance with resources required for the users. It is also shown that for the proposed designs the parametrization on the receiver side can be different from the transmitter side without considerable performance degradation.

Next in Section II, the fast-convolution filter bank (FC-FB) idea is reviewed and analytical models for the FC based synthesis and analysis FBs are derived. In Section III, its application to filtered OFDM is presented and the analytical models for the IBI and OBE are described. Numerical examples are given in Section IV, where the filtering performance and computational complexity with different parametrizations are demonstrated. Finally, the conclusions are drawn in Section V.

II. Fast-Convolution Filter Banks

This paper uses a special implementation scheme for multirate filters and FBs which is based on FC processing. The main idea is that a high-order filter can be implemented effectively through multiplication in frequency domain, after taking

This work was partially supported by the Finnish Funding Agency for Technology and Innovation (Tekes) and Nokia Bell Labs, under the projects "Phoenix+" and "5G Radio Systems Research".

The extended version of this paper was published in *IEEE Journal on Selected Areas in Communications* [1].

discrete Fourier transforms (DFTs) of the input sequence and the filter impulse response. The time-domain output signal is obtained by inverse discrete Fourier transform (IDFT). In practice, efficient implementation techniques, like fast Fourier transforms (FFT/IFFT), are used for the transforms, and overlap-save processing is applied for long sequences.

The application of FC to multirate filters has been presented in [9], and FC implementations of channelization filters have been considered in [10]–[12]. The authors have introduced the idea of FC-implementation of nearly perfect-reconstruction FB systems and detailed analysis and FC-FB optimization methods are developed in [13], [14]. In [15] FC approach has been applied for filter bank multicarrier (FBMC) waveforms and in [16] for flexible single-carrier (SC) waveforms. These papers demonstrate the flexibility and efficiency of FC-FB in communication signal processing.

A. Fast-Convolution Filtering Schemes

Fig. 1(a) shows the structure of FC-based flexible synthesis FB, for a case where the M incoming low-rate, narrowband signals $\mathbf{x}_m$, for $m = 0, 1, \ldots, M-1$, with adjustable frequency responses and adjustable sampling rates are to be combined into single wideband signal $\mathbf{y}$. The dual structure shown in Fig. 1(b) can be used on the receiver side as an analysis FB for splitting the incoming high-rate, wideband signal into several narrowband signals [17].

In the synthesis FB case, each of the M incoming signals is first segmented into overlapping blocks of length L_m for $m = 0, 1, \ldots, M-1$. Then, each input block is transformed to frequency-domain using DFT of length L_m. The frequency-domain bin values of the converted signal are multiplied by the weight values corresponding to the DFT of the finite-length linear filter impulse response, $[\mathbf{d}_m]_\ell = \sum_{n=0}^{L_m-1} h_m[n] \mathrm{e}^{-\mathrm{j}2\pi(\ell+L_m/2)n/L_m}$ for $m = 0, 1, \ldots, M-1$ and $\ell = 0, 1, \ldots, L_m - 1$.[1] Here, $h_m[n]$ is the impulse response of the prototype filter, m is the subband index and ℓ is the DFT bin index within the subband. Finally, the weighted signals are combined and converted back to time-domain using IDFT of length N and the resulting time-domain output blocks are concatenated using the overlap-save principle [18], [19].

The multirate FC-processing of Fig. 1(a) increases the sampling rates of the subband signals by the factors of

$$I_m = N/L_m = N_\mathrm{S}/L_{\mathrm{S},m}, \tag{1}$$

where $L_{\mathrm{S},m}$ and N_S are the number of non-overlapping input and output samples, respectively. The number of overlapping samples $L_{\mathrm{O},m} = L_m - L_{\mathrm{S},m}$ is divided into leading and tailing overlapping parts as follows:

$$L_{\mathrm{L},m} = \lceil (L_m - L_{\mathrm{S},m})/2 \rceil \text{ and } L_{\mathrm{T},m} = \lfloor (L_m - L_{\mathrm{S},m})/2 \rfloor. \tag{2}$$

Given the IDFT length N, the sampling rate conversion factor is determined by the DFT length L_m, and it can be configured for each subband individually. Naturally, L_m determines the maximum number of non-zero frequency bins, i.e., the bandwidth of the subband.

[1] For convenience of notation, we use the "FFT-shifted" indexing scheme in this context, i.e., index 0 corresponds to the lower edge of the subband

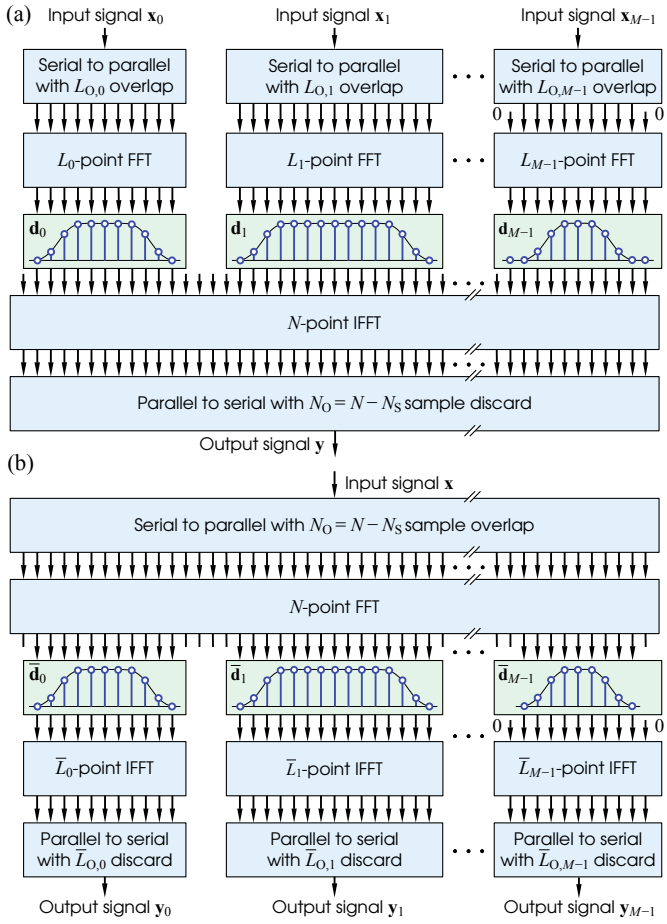

Fig. 1. (a) FC based flexible synthesis FB structure. (b) Corresponding FC analysis FB structure. The $\mathbf{d}_m$'s and $\bar{\mathbf{d}}_m$'s are the frequency-domain weights of the subband m for the synthesis and analysis FBs, respectively.

Regardless of the specific processing applied for each subband, the interpolation factor of the structure of Fig. 1(a) is given by (1) [9]. This means that the length of the FC output block is increased by the same factor, and so is also the length of the overlapping part in the overlap-save processing. The input and output block lengths have to exactly match, taking into account the sampling rate conversion factor. Generally, $N = p\Gamma$ and $N_\mathrm{S} = q\Gamma$, where p and q are two relatively prime integers and $\Gamma = \gcd(N, N_\mathrm{S})$, where $\gcd(\cdot)$ is the greatest common divisor. Then for narrowest possible subband case satisfying the integer-length criterion, $L_m = p$ and $L_{\mathrm{S},m} = q$. Generally, L_m has to be a multiple of N/Γ, that is, the configurability of the output sampling rate depends greatly on the choice of N and N_S.

In the analysis FB case, it is assumed that the forward transform size is larger than the inverse transform sizes and, therefore, the above process reduces the sampling rate of the subband signal by factors of

$$D_m = N/\bar{L}_m = N_\mathrm{S}/\bar{L}_{\mathrm{S},m}. \tag{3}$$

Here, the IDFT lengths on the analysis FB side are denoted by $\bar{L}_m$'s. For simplicity, it is assumed that the long transform size N for synthesis and analysis FBs is the same.

In [13], the performance of the FC-FB is analyzed using a periodically time-variant model and effective tools for frequency response analysis and FC-FB optimization are developed. It is also shown that the complexity of the FC-FB is considerably smaller when compared with the traditional polyphase implementations of FBMC [13].

B. Linear Periodically Shift Variant Model of the FC-FB

In the FC synthesis FB case, the block processing of mth subband signal $\mathbf{x}_m$ can be represented as

$$\mathbf{w}_m = \mathbf{F}_m \mathbf{x}_m, \tag{4a}$$

where $\mathbf{F}_m$ is the block diagonal transform matrix of the form

$$\mathbf{F}_m = \mathrm{diag}(\mathbf{F}_{m,0}, \mathbf{F}_{m,1}, \ldots, \mathbf{F}_{m,R_m-1}) \tag{4b}$$

with R_m blocks. Here, the dimensions and locations of the $\mathbf{F}_{m,r}$'s are determined by the overlapping factor of the overlap-save processing as defined as

$$\lambda = 1 - L_{\mathrm{S},m}/L_m = 1 - N_\mathrm{S}/N, \tag{5}$$

where $L_{\mathrm{S},m}$ and N_S are the number of non-overlapping input and output samples, respectively.

The multirate version of the FC synthesis FB can be represented using block processing by decomposing the $\mathbf{F}_{m,r}$'s as the following $N_\mathrm{S} \times L_m$ matrix

$$\mathbf{F}_{m,r} = \mathbf{S}_N \mathbf{W}_N^{-1} \mathbf{M}_{m,r} \mathbf{D}_m \mathbf{P}_{L_m}^{(L_m/2)} \mathbf{W}_{L_m}. \tag{6}$$

Here, $\mathbf{W}_{L_m}$ and $\mathbf{W}_N^{-1}$ are the $L_m \times L_m$ DFT matrix (with $[\mathbf{W}_{L_m}]_{p,q} = \mathrm{e}^{-\mathrm{j}2\pi(p-1)(q-1)/L_m}$) and $N \times N$ inverse DFT matrix, respectively. The DFT shift matrix $\mathbf{P}_{L_m}^{(L_m/2)}$ is circulant permutation matrix obtained by cyclically left shifting the $L_m \times L_m$ identity matrix by $L_m/2$ positions. $\mathbf{D}_m$ is the $L_m \times L_m$ diagonal matrix with the frequency-domain weights of the subband m on its diagonal whereas $\mathbf{M}_{m,r}$ and $\mathbf{S}_N$ are the frequency-domain mapping and time-domain selection matrices, respectively. The $N \times L_m$ frequency-domain mapping matrix maps L_m frequency-domain bins of the input signal to frequency-domain bins $(c_m - \lceil L_m/2 \rceil + \ell)_N$ for $\ell = 0, 1, \ldots, L_m - 1$ of output signal. Here c_m is the center bin of the subband m and $(\cdot)_N$ denotes the modulo-N operation. In addition, this matrix rotates the phases of the block by

$$\theta_m(r) = \exp(\mathrm{j}2\pi r \theta_m) \quad \text{with} \quad \theta_m = c_m L_{\mathrm{S},m}/L_m \tag{7}$$

in order to maintain the phase continuity between the consecutive overlapping processing blocks. The $N_\mathrm{S} \times N$ selection matrix $\mathbf{S}_N$ selects the desired N_S output samples from the inverse transformed signal corresponding to overlap-save processing.

In the analysis FB case, the corresponding analysis sub-block matrix of size $\bar{L}_{\mathrm{S},m} \times N$ can be decomposed as

$$\mathbf{G}_{m,r} = \mathbf{S}_{\bar{L}_m} \mathbf{W}_{L_m}^{-1} \mathbf{P}_N^{(N/2)} \mathbf{D}_m \mathbf{M}_{m,r}^\mathsf{T} \mathbf{W}_N, \tag{8}$$

where $\mathbf{P}_N^{(N/2)}$ is the inverse Fourier-shift matrix and the $\bar{L}_{\mathrm{S},m} \times L_m$ selection matrix $\mathbf{S}_{\bar{L}_m}$ selects the desired $\bar{L}_{\mathrm{S},m}$ output samples from the inverse transformed output signal.

In our approach, FC design is done in frequency-domain by defining/optimizing the weight coefficients. Generally, the frequency-domain weights consist of two symmetric transition bands with non-trivial weights. All passband weights are set to one, and all stopband weights are set to zero. The number of stopband weights can be selected to reach a feasible subband oversampling factor. Fig. 1 shows the typical weights for the cases with different bandwidths.

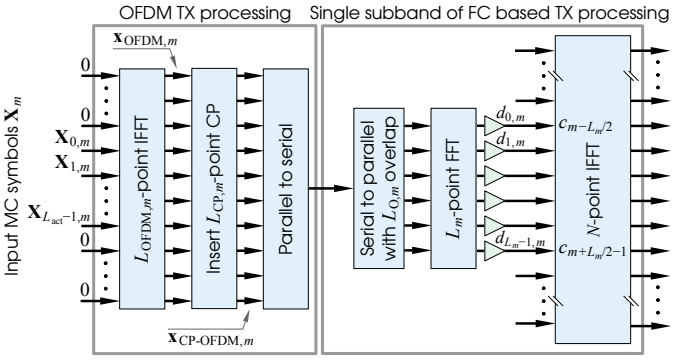

Fig. 2. FC-FB based processing for filtered OFDM transmitter. The processing structure for one filter channel group of PRBs is shown. The long N-point IFFT is common for all filter bank channels (c.f. Fig. 1(a)).

III. FC BASED FILTERED OFDM

We apply FC-FB for physical resource block (PRB) level filtering, while utilizing normal CP-OFDM waveform for the PRBs [7], [8]. One application is in cellular uplink scenarios, in which the different user equipments (UEs) utilize different PRBs for their transmissions. UEs may utilize single-channel FC-filtering, or corresponding time-domain filtering to shape their spectra. For good isolation of different users' PRBs, a few subcarriers are needed as guardbands between the PRBs. Good OBE characteristics allow to relax the tight synchronization requirements of traditional uplink multiuser orthogonal frequency-division multiple access (OFDMA). On the base-station side, a FC-based analysis FB is used for separating the PRBs of different UEs. Furthermore, it becomes possible to parametrize the waveforms differently for different UEs, e.g., using different subcarrier spacings (SCSs), CP-lengths, and/or frame structures [8]. Concerning cellular downlink scenarios, synchronization is not an issue, but the filtered OFDM idea would still make it possible to parametrize individually different users' signals in different groups of PRBs.

With FC-FB, it is easy to adjust the filtering bandwidth for the subbands individually. This is very useful in PRB-filtered OFDM because there is no need to realize filter transition bands and guardbands between equally parametrized synchronous PRBs. In the extreme case, the group of filtered PRBs could cover the full carrier bandwidth, and FC filtering would implement tight channelization filtering for the whole carrier.

Fig. 2 shows a block diagram of a FC-filtered OFDM base-station transmitter. In [7], it was assumed that the short fast Fourier transform (FFT)-length in FC processing is the same as the IFFT length in OFDM processing. In [8], this constraint is relaxed and it is assumed that the two transform lengths can be chosen independently. In our earlier model, the FFT-domain filtering weights correspond to the OFDM subcarriers,

but in the new model such direct connection is not necessary anymore.

In the structure of Fig. 2, the OFDM processing module generates useful symbol duration of $L_{\mathrm{OFDM},m}$ with the CP length of $L_{\mathrm{CP},m}$. The FC-filtering process increases the sampling rate by the factor of N/L_m, resulting in overall symbol duration of $N_{\mathrm{OVR}} = N_{\mathrm{OFDM}} + N_{\mathrm{CP}} = N/L_m(L_{\mathrm{OFDM},m} + L_{\mathrm{CP},m})$. Here $L_{\mathrm{OFDM},m}$ and $L_{\mathrm{CP},m}$ need to take integer values. It is convenient, but not necessary, that N_{OFDM} and N_{CP} take integer values as well. The FC's long transform length N is assumed to be fixed in the following discussions.

A. FC-filtered OFDM transmultiplexer optimization

The CP-OFDM processing of the mth OFDM subchannel on the transmitter side can be expressed as

$$\mathbf{T}_{\mathrm{TX},m} = \mathbf{T}_{\mathrm{CP},m}\mathbf{W}^{-1}_{\mathrm{OFDM},m}, \tag{9a}$$

where $\mathbf{W}^{-1}_{\mathrm{OFDM},m}$ is the $L_{\mathrm{OFDM},m} \times L_{\mathrm{OFDM},m}$ IDFT matrix and the $(L_{\mathrm{OFDM},m}+L_{\mathrm{CP},m}) \times L_{\mathrm{OFDM},m}$ CP insertion matrix is given by

$$\mathbf{T}_{\mathrm{CP},m} = \left[\begin{bmatrix}\mathbf{0}_{L_{\mathrm{CP},m}\times(L_{\mathrm{OFDM},m}-L_{\mathrm{CP},m})} & \mathbf{I}_{L_{\mathrm{CP},m}}\end{bmatrix}^{\mathsf{T}} \quad \mathbf{I}_{L_{\mathrm{OFDM},m}}\right]^{\mathsf{T}}. \tag{9b}$$

Here, $\mathbf{0}_{q\times p}$ and $\mathbf{I}_r$ are $q \times p$ zero matrix and $r \times r$ identity matrix, respectively. The impulse response from the ℓth OFDM subcarrier on subchannel m to the FC-FB output can be expressed as

$$\mathbf{f}^{(\mathrm{OFDM})}_{\ell,m} = \mathbf{F}^{(\mathrm{sub})}_m \mathbf{T}_{\mathrm{TX},m}\begin{bmatrix}\mathbf{0}_{1\times\ell-1} & 1 & \mathbf{0}_{1\times L_{\mathrm{OFDM},m}-\ell}\end{bmatrix}^{\mathsf{T}}, \tag{10a}$$

where the $P_m \times (L_{\mathrm{OFDM},m}+L_{\mathrm{CP},m})$ sub-matrix $\mathbf{F}^{(\mathrm{sub})}_m$ with $P_m = N_{\mathrm{S}}B_{\mathrm{F},m}$ and $B_{\mathrm{F},m} = \lceil (L_{\mathrm{OFDM},m}+L_{\mathrm{CP},m})/L_{\mathrm{S},m} \rceil$ is obtained by selecting the desired rows and columns from $\mathbf{F}_m$ as follows:

$$[\mathbf{F}^{(\mathrm{sub})}_m]_{p,q} = [\mathbf{F}_m]_{p,q+S_{\mathrm{F},m}} \tag{10b}$$

with $S_{\mathrm{F},m} = L_{\mathrm{O},m} = L_m - L_{\mathrm{S},m}$ for $p = 1, 2, \ldots, P_m$ and for $q = 1, 2, \ldots, L_{\mathrm{OFDM},m} + L_{\mathrm{CP},m}$.

On the receiver side the OFDM processing can be expressed as

$$\mathbf{T}_{\mathrm{RX},m} = \mathbf{W}_{\mathrm{OFDM},m}\mathbf{R}_{\mathrm{CP},m}, \tag{11a}$$

where $\mathbf{W}_{\mathrm{OFDM},m}$ is the $\bar{L}_{\mathrm{OFDM},m} \times \bar{L}_{\mathrm{OFDM},m}$ DFT matrix and the $(\bar{L}_{\mathrm{OFDM},m}+\bar{L}_{\mathrm{CP},m}) \times \bar{L}_{\mathrm{OFDM},m}$ CP removal matrix is given by

$$\mathbf{R}_{\mathrm{CP},m} = \begin{bmatrix}\mathbf{0}_{\bar{L}_{\mathrm{OFDM},m}\times\bar{L}_{\mathrm{CP},m}} & \mathbf{I}_{\bar{L}_{\mathrm{OFDM},m}}\end{bmatrix}. \tag{11b}$$

Now the impulse response from the FC-FB input to the ℓth OFDM subcarrier can be expressed as

$$\mathbf{G}^{(\mathrm{OFDM})}_{\ell,m} = \mathbf{C}^{(\ell)}_m \mathbf{T}^{(\mathrm{diag})}_{\mathrm{RX},m}\mathbf{G}^{(\mathrm{sub})}_m, \tag{12a}$$

where the $Q_m \times P_m$ sub-matrix $\mathbf{G}^{(\mathrm{sub})}_m$ with $Q_m = \bar{L}_{\mathrm{S},m}B_{\mathrm{G},m}$ and $B_{\mathrm{G},m} = \lfloor (P_m + N)/N_{\mathrm{S}} - (B_{\mathrm{F},m})_2 \rfloor$ is given by

$$[\mathbf{G}^{(\mathrm{sub})}_m]_{q,p} = [\mathbf{G}_m]_{q,p+S_{\mathrm{G},m}} \tag{12b}$$

with $S_{\mathrm{G},m} = \lfloor (N + [B_{\mathrm{G},m} - 1]N_{\mathrm{S}} - P_m)/2 \rfloor$ for $q = 1, 2, \ldots, Q_m$ and for $p = 1, 2, \ldots, P_m$. The block diagonal $Q_m \times Q_m$ matrix $\mathbf{T}^{(\mathrm{diag})}_{\mathrm{RX},m}$ is constructed from block diagonal $B_{\mathrm{OFDM},m}\bar{L}_{\mathrm{OFDM},m} \times B_{\mathrm{OFDM},m}(\bar{L}_{\mathrm{OFDM},m} + \bar{L}_{\mathrm{CP},m})$ matrix with $B_{\mathrm{OFDM},m} = \lceil Q_m/(\bar{L}_{\mathrm{OFDM},m} + \bar{L}_{\mathrm{CP},m}) \rceil$ blocks

$$\widehat{\mathbf{T}}^{(\mathrm{diag})}_{\mathrm{RX},m} = \mathrm{diag}(\underbrace{\mathbf{T}_{\mathrm{RX},m}, \mathbf{T}_{\mathrm{RX},m}, \ldots, \mathbf{T}_{\mathrm{RX},m}}_{B_{\mathrm{OFDM},m}\text{ blocks}}) \tag{13}$$

by selecting the first Q_m rows and columns whereas $\mathbf{C}^{(\ell)}_m$ is the $Q_m \times Q_m$ down-sampling by $\bar{L}_{\mathrm{OFDM},m}$ with ℓ-sample offset matrix.

For this model, the overall transfer function from the OFDM subcarrier ℓ to subcarrier $\acute{k}$ is expressed as

$$\mathbf{t}^{(m,n)}_{\ell,\acute{k}} = \mathbf{G}^{(\mathrm{OFDM})}_{\acute{k},n}\mathbf{f}^{(\mathrm{OFDM})}_{\ell,m}. \tag{14}$$

Stemming from the above fundamental modeling, the mean-squared IBI from the OFDM subcarrier ℓ of subband m to subcarrier $\acute{k}$ of subband n can be expressed as

$$\varepsilon^{(m)}_{\mathrm{IBI},\ell} = \frac{1}{E_{\mathrm{s}}}\left[\left\|\mathbf{e} - \mathbf{t}^{(m,m)}_{\ell,\ell}\right\|^2 + \sum_{\acute{k}=0,\acute{k}\neq\ell}^{\bar{L}_{\mathrm{act},m}-1}\left\|\mathbf{t}^{(m,m)}_{\ell,\acute{k}}\right\|^2\right], \tag{15}$$

where $\mathbf{e} = [\mathbf{0}_{1\times U_m} \quad 1 \quad \mathbf{0}_{1\times V_m}]^{\mathsf{T}}$ with $U_m = \lceil S_{\mathrm{G},m}\bar{L}_m/(N\bar{L}_{\mathrm{OFDM},m}) \rceil$ and $V_m = \lceil P_m/\bar{L}_{\mathrm{OFDM},m} \rceil - U_m$, $\bar{L}_{\mathrm{act},m}$ is number of active subcarriers on the receiver side on subchannel m, and E_{s} is the energy per symbol. Here, the first term measures the effect of time-domain dispersion at subcarrier index ℓ, resulting in general into inter-symbol interference (ISI) between U_m preceding and V_m following OFDM symbols. The second term, in turn, contains the inter-carrier interference (ICI) induced by the desired symbol, U_m preceding symbols, and V_m following OFDM symbols.

In this contribution, we have used the minimum stopband attenuation as a figure of merit for the OBE since the spectral containment is typically expressed with the aid of spectrum emission masks. Therefore, the OBE characteristic can be directly evaluated from the impulse responses of the FC synthesis FB as given by (6).

The FC-filtered OFDM system design can now be stated as a problem for finding the optimal values of the frequency-domain window (diagonal of $\mathbf{D}_m$ in (6) and (8)) to minimize the maximum of the $\varepsilon^{(m)}_{\mathrm{IBI},\ell}$ for $\ell = 0, 1, \ldots, \bar{L}_{\mathrm{act},m} - 1$ subject to the constraint that the OBE is below the given limit. This problem can be straightforwardly solved using non-linear optimization algorithms since the number of parameters for the optimization is typically around ten when taking into account that only the transition band weights are used in the optimization.

IV. Numerical Examples

Example 1: We focus here on a 10 MHz long-term evolution (LTE) like multicarrier system utilizing OFDM waveform and using FC based synthesis and analysis FBs. The long transform length on the transmitter and receiver side is fixed to $N = 1024$. The sampling rate is $f_{\mathrm{s}} = 15.36$ MHz with $N_{\mathrm{OFDM}} = N = 1024$ and $N_{\mathrm{CP}} = 72$. This corresponds to the LTE numerology, leading to $\Delta f = 15$ kHz SCS. The number of active subcarriers on the transmitter side is $L_{\mathrm{act},m} = 600$. These active subcarriers are scheduled in PRBs of 12 subcarriers, i.e., there are 50

TABLE II. RX MEAN-SQUARED ERROR (MSE) VERSUS COMPLEXITY FOR DIFFERENT VALUES OF OVERLAP FACTOR IN EXAMPLE 1

No. active subcarriers	Overlap factor λ	Average inband MSE $A_s = 20\,\text{dB}$ ($A_s = 40\,\text{dB}$)	Worst-case inband MSE $A_s = 20\,\text{dB}$ ($A_s = 40\,\text{dB}$)	Rx complexity (muls/MC-symbol)	Rx complexity (muls/symbol)	Rx complexity relative to OFDM
1 PRB	1/2	−24.24 dB (−23.76 dB)	−23.22 dB (−22.57 dB)	17302	1441.83	×2.41
	1/4	−24.15 dB (−22.92 dB)	−23.12 dB (−21.30 dB)	11758	979.83	×1.64
4 PRB	1/2	−29.26 dB (−28.89 dB)	−24.78 dB (−23.89 dB)	17302	360.46	×2.41
	1/4	−29.31 dB (−28.32 dB)	−24.62 dB (−22.75 dB)	11758	244.96	×1.64
50 PRB	1/2	−40.93 dB (−40.41 dB)	−31.64 dB (−30.03 dB)	38468	64.11	×5.36
	1/4	−40.43 dB (−39.35 dB)	−30.57 dB (−26.12 dB)	28131	46.89	×3.92

TABLE I. EXAMPLE PARAMETRIZATIONS FOR FC-F-OFDM BASED 5G PHYSICAL LAYER WITH 10 MHz CARRIER BANDWIDTH

SCS	No. act. subcarr.	N	$\bar{L}_{\text{OFDM},m}$	$\bar{L}_m$	$\bar{L}_{\text{CP},m}$
15 kHz	12 (1 PRB)	1024	128	128	9
15 kHz	48 (4 PRBs)	1024	128	128	9
15 kHz	600 (50 PRBs)	1024	1024	1024	72
30 kHz	12 (1 PRB)	1024	128	256	9
30 kHz	24 (2 PRBs)	1024	128	256	9
30 kHz	300 (25 PRBs)	1024	512	1024	36
60 kHz	12 (1 PRB)	1024	128	512	9
60 kHz	72 (6 PRBs)	1024	128	512	9
60 kHz	144 (12 PRBs)	1024	256	1024	18

PRBs. We use transition bandwidths of six FFT bins, based on the results of [7].

On the receiver side, we are interested in receiving allocations of either 1, 4, or 50 PRBs. The minimum transform sizes needed for satisfying the integer criterion for the short transform CP lengths are tabulated in Table I. The required stopband attenuation for the synthesis FB in the optimization is either $A_s = 20\,\text{dB}$ or $A_s = 40\,\text{dB}$.

The simulation results giving in-band MSE, attenuation characteristic, and complexity evaluations are shown in Table II. In these simulations, the IBI is measured by the MSE in the equalized subcarrier symbols in reference to the symbol energy, and without channel noise. As can be seen from this table, the worst-case IBI is the lowest for the 50 PRB case and highest for the 1 PRB case. This is obviously due to the fact that on the edge subcarriers the strict orthogonality is impaired and its contribution to overall IBI is more severe for narrowband processing.

In addition, reducing the overlap factor from $\lambda = 1/2$ to $\lambda = 1/4$ has a quite small effect on the in-band MSE, however, the reduction in computational complexity is roughly 30 %. Furthermore, when comparing the computational complexities it can be observed that the number of multiplications per multicarrier (MC) symbol is reduced more than 55 % if only part of the transmitted subcarriers are to be received.

The power spectral density (PSD) plots for FC filtered OFDM signal with 50 active PRBs are shown in the upper sub-figure of Fig. 3. In this figure, the overlap factor in FC processing is $\lambda = 1/4$ and the required stopband attenuation is 40 dB. The lower sub-figure shows the simulated MSE on active subcarriers as well as the frequency-domain response of the analysis FBs.

Example 2: Here, the system is the same as in Example 1 except that the SCS can be configured to be either 15 kHz, 30 kHz, or 60 kHz. The feasible transform sizes are tabulated in Table I. In this case, only the designs with stopband attenuation of $A_s = 20\,\text{dB}$ are considered. Table III gives the simulated in-band MSEs for the optimized single PRB designs as well as the corresponding receiver complexities when compared with the basic CP-OFDM processing. As seen from this table, the MSE increases with the increasing SCS. The is because the transition band with respect to SCS reduces to 50 % or 25 % for the SCSs of 30 kHz and 60 kHz, respectively.

TABLE III. RX MSE VERSUS COMPLEXITY FOR DIFFERENT VALUES OF OVERLAP FACTOR IN EXAMPLE 2 IN THE CASE OF ONE PRB

SCS	Overlap factor λ	Average inband MSE	Worst-case inband MSE	Rx complexity relative to OFDM
15 kHz	1/2	−32.79 dB	−32.39 dB	×2.41
	1/4	−31.79 dB	−31.22 dB	×1.64
30 kHz	1/2	−30.31 dB	−29.49 dB	×2.67
	1/4	−30.12 dB	−28.89 dB	×1.82
60 kHz	1/2	−28.04 dB	−26.26 dB	×3.22
	1/4	−27.63 dB	−25.80 dB	×2.19

In the single PRB case, the in-band MSE level is sufficient for supporting 16-QAM modulation and possibly 64-QAM modulation, depending on the OBE attenuation requirements and overlap factor. Typically, single PRB transmissions are used only on cell edge in coverage limited scenarios where the used modulation is most likely QPSK and not limited by the FC processing induced in-band MSE.

The PSD plots for the FC filtered OFDM signal with three RBGs of $N_{\text{act}} = \{12, 72, 288\}$ active subcarriers with SCSs of $\{30, 60, 15\}$ kHz, respectively, are shown in the upper sub-figure of Fig. 4. Here, the overlap factor in FC processing is $\lambda = 1/2$. The lower sub-figure shows the simulated MSE on active subcarriers as well as the frequency-domain responses of the analysis FBs.

V. CONCLUSIONS

We have proposed a straightforward technique for optimizing the performance of the FB based OFDM processing such that the IBI can be minimized with respect to the constraints on the OBE. The performance of the optimized designs and the trade-offs between the implementation complexities, IBI, and the spectral emission are demonstrated using an example.

The presented performance and complexity evaluations show that FC based subband/RBG filtering is computationally efficient solution especially for UE side in the case of narrow

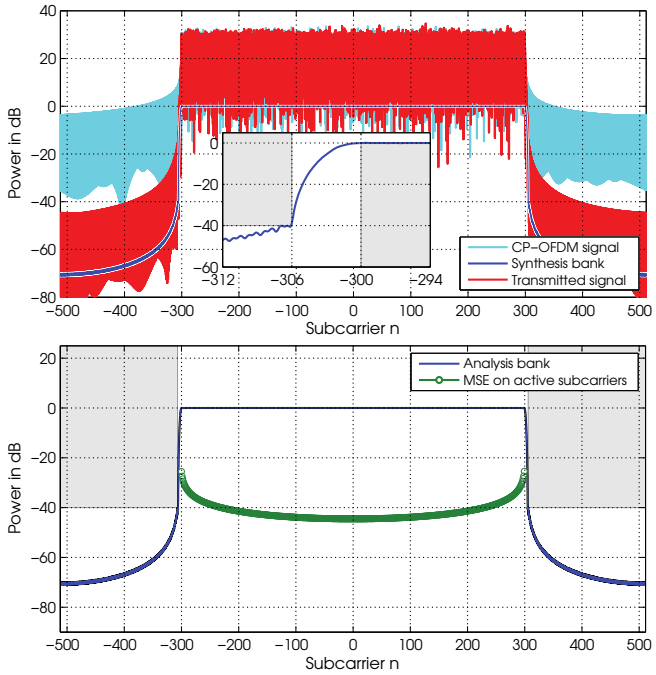

Fig. 3. Upper figure: PSD of the generated FC-filtered OFDM signal in the case of 50 active PRBs. The overlap factor for FC processing is $\lambda = 1/4$ and the required stopband attenuation is 40 dB. Lower figure: Simulated in-band subcarrier MSE in the case of 50 active PRBs.

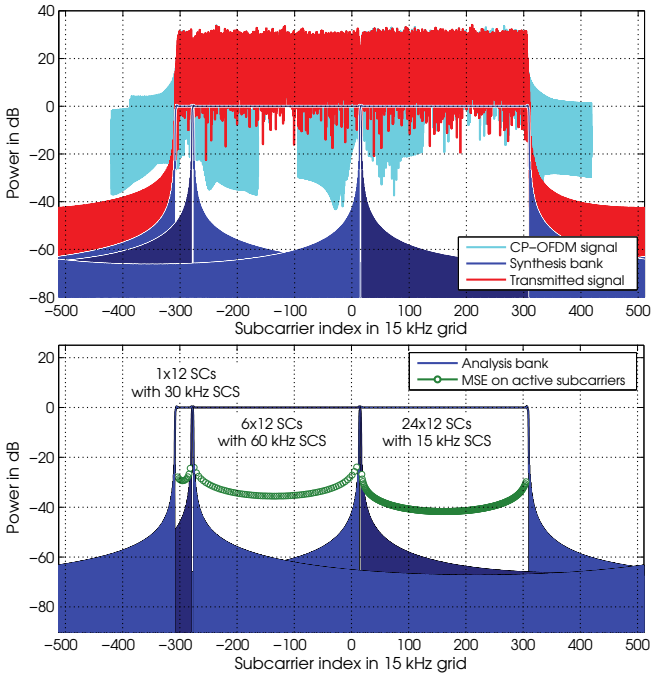

Fig. 4. Upper figure: PSD of the generated FC-filtered OFDM signal in the case of three RBGs of $N_{\text{act}} = \{12, 72, 288\}$ active subcarriers with SCSs of $\{30, 60, 15\}$ kHz, respectively. The overlap factor for FC processing is $\lambda = 1/2$ and the required stopband attenuation is 20 dB. Lower figure: Simulated in-band subcarrier MSE.

band allocation, but also for wide band filtering in base-station and UE side. The overlap factor of 1/4 provides significant complexity savings with modest impact on the inband MSE with optimized filter designs, and can be considered as the most interesting option for implementation.

REFERENCES

[1] J. Yli-Kaakinen, T. Levanen, S. Valkonen, K. Pajukoski, J. Pirskanen, M. Renfors, and M. Valkama, "Efficient fast-convolution based waveform processing for 5G physical layer," *IEEE J. Select. Areas Commun.*, vol. 35, no. 8, pp. 1–18, Aug. 2017.

[2] A. Toskala and H. Holma, Eds., *LTE for UMTS – OFDMA and SC-FDMA Based Radio Access*. Wiley, 2009.

[3] *R1-167963, Way Forward on Waveform*, document TSG-RAN WG1 Meeting #86, 3GPP, 2016.

[4] F. Schaich, T. Wild, and Y. Chen, "Waveform contenders for 5G – Suitability for short packet and low latency transmissions," in *Proc. Veh. Technol. Conf. (VTC Spring)*, May 2014, pp. 1–5.

[5] J. Abdoli, M. Jia, and J. Ma, "Filtered OFDM: A new waveform for future wireless systems," in *Proc. Int. Workshop on Signal Process. Advances in Wireless Commun. (SPAWC)*, Jun. 2015, pp. 66–70.

[6] J. Li, E. Bala, and R. Yang, "Resource block filtered-OFDM for future spectrally agile and power efficient systems," *Physical Communication*, vol. 14, pp. 36–55, Jun. 2014.

[7] M. Renfors, J. Yli-Kaakinen, T. Levanen, M. Valkama, T. Ihalainen, and J. Vihriälä, "Efficient fast-convolution implementation of filtered CP-OFDM waveform processing for 5G," in *Proc. Globecom Workshops*, San Diego, CA, USA, Dec. 2015.

[8] M. Renfors, J. Yli-Kaakinen, T. Levanen, and M. Valkama, "Fast-convolution filtered OFDM waveforms with adjustable CP length," in *Proc. Global Conf. on Signal and Inform. Process. (GlobalSIP)*, Greater Washington, D.C., USA, 2016.

[9] M. Borgerding, "Turning overlap-save into a multiband mixing, downsampling filter bank," *IEEE Signal Processing Mag.*, pp. 158–162, Mar 2006.

[10] M.-L. Boucheret, I. Mortensen, and H. Favaro, "Fast convolution filter banks for satellite payloads with on-board processing," *IEEE J. Select. Areas Commun.*, vol. 17, no. 2, pp. 238–248, Feb. 1999.

[11] C. Zhang and Z. Wang, "A fast frequency domain filter bank realization algorithm," in *Proc. Int. Conf. Signal Process.*, vol. 1, Beijing, China, Aug. 2000, pp. 130–132.

[12] L. Pucker, "Channelization techniques for software defined radio," in *Proc. Software Defined Radio Tech. Conf. (SDR)*, Orlando, FL, USA, Nov. 18–19 2003.

[13] M. Renfors, J. Yli-Kaakinen, and F. Harris, "Analysis and design of efficient and flexible fast-convolution based multirate filter banks," *IEEE Trans. Signal Processing*, vol. 62, no. 15, pp. 3768–3783, Aug. 2014.

[14] J. Yli-Kaakinen and M. Renfors, "Optimized reconfigurable fast convolution based transmultiplexers for flexible radio access," *IEEE Trans. Circuits Syst. II*, pp. 1–5, 2017, to be published.

[15] K. Shao, J. Alhava, J. Yli-Kaakinen, and M. Renfors, "Fast-convolution implementation of filter bank multicarrier waveform processing," in *Proc. Int. Symp. on Circuits and Systems (ISCAS)*, Lisbon, Portugal, May 2015, pp. 978–981.

[16] M. Renfors and J. Yli-Kaakinen, "Flexible fast-convolution implementation of single-carrier waveform processing," in *Proc. Int. Conf. on Commun. Workshops (ICCW)*, London, UK, Jun. 2015, pp. 1243–1248.

[17] J. Yli-Kaakinen and M. Renfors, "Optimization of flexible filter banks based on fast convolution," *Journal of Signal Processing Systems*, vol. 85, no. 1, pp. 101–111, Aug. 2016.

[18] L. R. Rabiner and B. Gold, *Theory and Application of Digital Signal Processing*. Englewood Cliffs, NJ: Prentice-Hall, 1975.

[19] A. Daher, E.-H. Baghious, G. Burel, and E. Radoi, "Overlap-save and overlap-add filters: Optimal design and comparison," *IEEE Trans. Signal Processing*, vol. 58, no. 6, pp. 3066–3075, Jun. 2010.